

Expression, purification and characterization of *Arabidopsis thaliana* acetohydroxyacid synthase

Alan K. CHANG and Ronald G. DUGGLEBY¹

Centre for Protein Structure, Function and Engineering, Department of Biochemistry, University of Queensland, Brisbane, QLD 4072, Australia

Acetohydroxyacid synthase (EC 4.1.3.18) is the enzyme that catalyses the first step in the synthesis of the branched-chain amino acids valine, leucine and isoleucine. The AHAS gene from *Arabidopsis thaliana* with part of the chloroplast transit sequence removed was cloned into the bacterial expression vector pT7-7 and expressed in the *Escherichia coli* strain BL21(DE3). The expressed enzyme was purified by an extensive procedure involving $(\text{NH}_4)_2\text{SO}_4$ fractionation followed by hydrophobic and anion-exchange chromatography. The purified enzyme appears as a single band on SDS/PAGE with a molecular mass of about 61 kDa. On gel filtration the enzyme is a dimer, migrating as a single peak with molecular masses of 109 and 113 kDa in the absence and presence of FAD respectively. Ion spray MS analysis yielded a mass of 63 864 Da. The enzyme has optimum activity in

the pH range 6.5–8.5 and exhibits absolute dependence on the three cofactors FAD, Mg^{2+} and thiamine diphosphate for activity. It displays negatively co-operative kinetics with respect to pyruvate concentration. A model was derived to explain the non-hyperbolic substrate-saturation curve, involving interaction between the active sites of the dimer. The K_m for the first active site was found to be 8.01 ± 0.66 mM; the K_m for the second active site could not be accurately determined but was estimated to be approx. 100 mM. The enzyme is insensitive to valine, leucine and isoleucine but is strongly inhibited by the sulphonylurea herbicide, chlorsulphuron, and the imidazolinone herbicide, imazapyr. Inhibition by both herbicides exhibits slow-binding kinetics, whereas chlorsulphuron also shows tight-binding inhibition.

INTRODUCTION

Acetohydroxyacid synthase (EC 4.1.3.18; AHAS; also known as acetolactate synthase) catalyses the first common step in the metabolic pathway leading to the biosynthesis of branched-chain amino acids [1]. AHAS catalyses the condensation of two molecules of pyruvate to form acetolactate in the biosynthesis of valine and leucine, or the condensation of pyruvate and 2-oxobutyrate to form acetohydroxybutyrate in the biosynthesis of isoleucine. Biochemical studies have shown that AHAS requires FAD, thiamine diphosphate (ThDP) and a bivalent metal ion, Mg^{2+} or Mn^{2+} , for activity [2,3]. The enzyme uses ThDP as the coenzyme in the condensation reactions, and Mg^{2+} is presumed to be required for the binding of ThDP to the enzyme, as it is for other ThDP-dependent enzymes [4]. The function of FAD is unclear as the enzyme does not catalyse a redox reaction.

AHAS is the site of action of four different classes of herbicide; sulphonylureas, imidazolinones, triazolopyrimidines and pyrimidyl(oxy)benzoates [5–8]. These herbicides may bind to the regulatory site on the enzyme [7]. Data obtained from the studies of the interaction of sulphometuron methyl and AHAS from *Salmonella typhimurium* suggested that the herbicide binds to the enzyme at a site near ThDP and FAD, and overlapping the pyruvate substrate site [9].

AHAS has been purified from bacteria, particularly the enteric bacteria [10–13]. It exists as a tetramer composed of two large and two small subunits with apparent molecular masses of 60 and 9–17 kDa respectively. In yeast and other fungi, AHAS is located in the mitochondria [14]. The yeast enzyme has been purified as a recombinant enzyme expressed in *Escherichia coli*

[15] but, because of the instability of the enzyme, the yield was extremely low and the final specific activity was little greater than the initial cell extract. Yeast AHAS has an extended N-terminal sequence that is not present in bacterial AHAS and is thought to act as a mitochondrial transit peptide [16].

Owing to the high lability and very low abundance, purification of AHAS from plant tissue is difficult and results in very low yields. So far the enzyme has been obtained in apparently pure form from barley [17] and wheat leaves [18] only. AHAS from *Arabidopsis thaliana* [19–21], tobacco [21] and oilseed rape [22] has been functionally expressed in bacteria but the enzyme was not purified. More recently, *Arabidopsis* AHAS has been expressed in *E. coli* and purified as a glutathione S-transferase (GST) fusion protein. After cleavage of the GST portion, a functional enzyme was obtained without the first 59 amino acids but with an additional glycine at the N-terminus [23]. Unfortunately, few data were presented on the purity of the final product or its enzymic properties. In this paper we describe the expression and purification of *Arabidopsis* AHAS from *E. coli* and some physical and biochemical properties of the enzyme.

MATERIALS AND METHODS

Materials

FAD, ThDP, BSA, dithiothreitol (DTT), PMSF, α -naphthol, creatine hydrate, sodium pyruvate and Tris were obtained from Sigma Chemical Co. Chlorsulphuron was kindly provided by Dr. H. Brown (Du Pont Agricultural Products), and imazapyr was a

Abbreviations used: AHAS, acetohydroxyacid synthase; DTT, dithiothreitol; GST, glutathione S-transferase; TFA, trifluoroacetic acid; ThDP, thiamine diphosphate.

¹ To whom correspondence should be addressed.

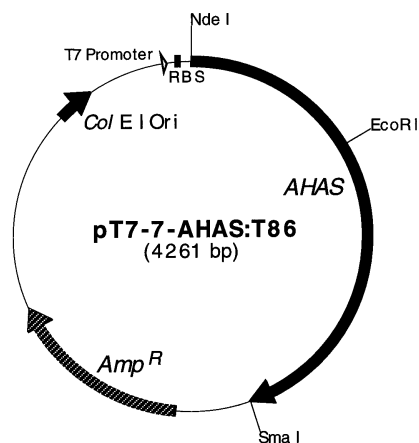


Figure 1 Map of the pT7-7-AHAS:T86 expression clone

gift from Dr. B. K. Singh (American Cyanamid). $(\text{NH}_4)_2\text{SO}_4$, KCl, MgCl_2 and potassium phosphate were purchased from Ajax. Phenyl-Sepharose CL-4B was obtained from Pharmacia. Macro-Prep 50 Q and gel-filtration molecular-mass standards were obtained from Bio-Rad. Restriction enzymes, T4 DNA ligase and Vent DNA polymerase were purchased from New England Biolabs.

E. coli strain BL21(DE3) [*hds gal* (λ Clts857 *ind1 Sam7 nin5 lacUV5-T7* gene 1)] was obtained from Novagen, and strain CU1147 was kindly provided by Dr. H. E. Umbarger, Purdue University. The expression vectors were obtained from United States Biochemical Corp. (pT7-7), Pharmacia (pTrc99A) and Dr. N. E. Dixon, Australian National University (pND216).

Construction of recombinant plasmids

The *Arabidopsis* AHAS gene [24] was obtained from Dr. B. Miki and Dr. J. Hattori (Plant Research Centre, Agriculture Canada) as the plasmid pALSTX containing a 5.5 kb fragment comprising the AHAS promoter region, the entire coding region and the 3'-non-coding region. The AHAS gene contains *NcoI* site at the first codon. Plasmid manipulation and expression generally followed the methodology outlined by Sambrook et al. [25].

pTrc99A derivatives

The plasmid pTrc99A-AHAS was constructed by cloning into *NcoI*–*SmaI* sites of pTrc99A, thereby removing all of the 5'-, and most of the 3'-non-coding regions. Addition of the coding sequence for a hexahistidine tag to pTrc99A-AHAS yielded pTrc99A-AHAS(H), and removal of the first 101 codons gave pTrc99A-AHAS:I102.

pND216-AHAS

This plasmid was obtained in a similar way to pTrc99A-AHAS, by cloning into pND216.

pT7-7 derivatives

The *NcoI* site of pALSTX was changed into an *NdeI* site by PCR, then the coding sequence was cloned into pT7-7 to give pT7-7-AHAS. For purification of AHAS, the gene was modified by PCR to remove the first 85 amino acids of the transit sequence. A 740 bp fragment DNA containing *NdeI* and *EcoRI*

sites was cut with these enzymes and cloned into the *NdeI*–*EcoRI* sites of pT7-7 to yield an intermediate construct. This intermediate construct has an additional methionine at the N-terminus of a truncated AHAS protein. The rest of the AHAS gene was cloned into the intermediate construct as an *EcoRI*–*SmaI* fragment excised from pTrc99A-AHAS, yielding pT7-7-AHAS:T86 (Figure 1).

Expression of AHAS

In small-scale expression trials, cells containing just the vector or vector with an AHAS insert were grown in 5 ml of 2YT broth [25] containing 100 $\mu\text{g/ml}$ ampicillin, and induced when the A_{600} reached 0.5–0.8. Cells containing plasmids derived from pT7-7 or pTrc99A were grown at 37 °C and induced by addition of 0.5 mM isopropyl β -D-thiogalactoside. Induction was carried out at 30 °C for 3 h. Cells harbouring the pND-216 vector with and without AHAS insert were grown at 30 °C and induced by raising the temperature to 42 °C for 3 h. AHAS activity was measured in the soluble fraction of cell lysate using the colorimetric assay (see below).

Purification of AHAS

For larger-scale expression of AHAS, pT7-7-AHAS:T86 was transformed into *E. coli* strain BL21(DE3) and cells harbouring the plasmid were grown overnight in 2YT broth containing 100 $\mu\text{g/ml}$ ampicillin. The overnight culture was diluted 1:25 into 500 ml of 2YT broth containing 100 $\mu\text{g/ml}$ ampicillin. The culture was grown at 37 °C with shaking until an A_{600} of approx. 0.8 was reached. Isopropyl thiogalactoside was added to the culture to a final concentration of 0.2 mM and the culture was incubated for 3 h at 30 °C. Enzyme was routinely purified from a 2-litre culture.

During purification, all operations were carried out at 4 °C unless otherwise stated. For every gram of wet cell paste of *E. coli* BL21(DE3)/pT7-7-AHAS:T86, 6 ml of lysis buffer (50 mM Tris/HCl, pH 7.5, 15% glycerol, 5 mM MgCl_2 , 1 mM EDTA, 1 mM DTT, 0.1 mM FAD, 0.1% Triton X-100, 0.2 mM PMSF, 0.2 mg/ml lysozyme, 10 $\mu\text{g/ml}$ DNase I) was added. This suspension was incubated with stirring at 4 °C for 45 min and then subjected to sonication for 8 \times 20 s at 90% duty cycle and 75 W, with 1 min rest intervals using a Branson sonic B-30 cell disrupter. Cell debris was removed by centrifugation at 17000 g for 20 min. Solid $(\text{NH}_4)_2\text{SO}_4$ was added to the supernatant to give a 30% satn. (176 g/l or 1.23 M). The precipitate was removed by centrifugation at 39000 g for 15 min and the supernatant was diluted with buffer B (50 mM Tris/HCl, pH 7.5, 15% glycerol, 5 mM MgCl_2 , 0.2 mM DTT, 10 μM FAD) to give a final $(\text{NH}_4)_2\text{SO}_4$ concentration of about 1 M. This solution was applied to a Phenyl-Sepharose CL-4B column (2.4 cm \times 10 cm) equilibrated in buffer A [buffer B plus 1 M $(\text{NH}_4)_2\text{SO}_4$]. After the column had been washed free of unbound proteins, it was eluted with a linear gradient consisting of 90 ml of buffer A and 90 ml of buffer B. Fractions containing AHAS activity were pooled and concentrated by precipitation with $(\text{NH}_4)_2\text{SO}_4$ (50% satn.) and centrifuged as described above. The precipitate was resuspended in buffer C (25 mM $\text{K}_2\text{HPO}_4/\text{KH}_2\text{PO}_4$, pH 7.5, 15% glycerol, 5 mM MgCl_2 , 0.2 mM DTT, 10 μM FAD) and desalted on a PD-10 column (Pharmacia) equilibrated with buffer C. The desalted protein solution was applied to a Macro-Prep 50 Q column (1.6 cm \times 20 cm) equilibrated with buffer C. After the column had been washed free of unbound proteins, it was eluted with 180 ml of buffer C containing a linear gradient of KCl (0–300 mM) at a flow rate of 0.6 ml/min. Fractions containing most of the AHAS activity were pooled, concentrated

and desalted as described above in buffer D (25 mM imidazole/HCl, pH 6.5, 15% glycerol, 5 mM MgCl₂, 0.2 mM DTT, 10 μM FAD). The desalted protein solution was applied to the same Macro-Prep 50 Q column equilibrated with buffer D. Elution of AHAS was achieved with 180 ml of buffer D containing a linear gradient of KCl (0–300 mM) at a flow rate of 0.6 ml/min. Fractions containing the majority of AHAS activity were pooled and stored in small aliquots at –70 °C. The enzyme preparation was used for biochemical study without further purification. For cofactor-saturation studies, the enzyme preparation was exchanged into a buffer containing 50 mM K₂HPO₄/KH₂PO₄ (pH 7.0), 15% glycerol, 0.2 mM DTT and 1 mM EDTA. All chromatography steps were carried out with minimal exposure to light, either in the dark or with equipment wrapped in aluminium foil.

AHAS assay and protein determination

AHAS activity was assayed by the method of Singh et al. [3] in a 250 μl reaction mixture containing 50 mM K₂HPO₄/KH₂PO₄, pH 7.0, 50 mM sodium pyruvate, 10 mM MgCl₂, 1 mM ThDP, 10 μM FAD and enzyme. The reaction mixture was incubated at 37 °C for 30 min and the reaction stopped with 25 μl of 10% H₂SO₄ and heated at 60 °C for 15 min to convert acetolactate into acetoin. The acetoin formed was quantified by incubation with creatine (0.17%, w/v) and α-naphthol (1.7%, w/v) for 15 min at 60 °C and A₅₂₅ was measured (ε_M = 22700 M⁻¹·cm⁻¹, determined using authentic acetoin). One unit of enzyme activity is defined as the production of 1 μmol of acetolactate/min in this reaction. AHAS activity was also measured using a continuous assay which monitors the consumption of pyruvate directly at 333 nm (ε_M = 17.5 M⁻¹·cm⁻¹ from [12]); standard assay conditions were identical with those used in the colorimetric assay except that the pyruvate concentration was 100 mM. All kinetic studies were performed using the continuous assay, with pyruvate, cofactors or inhibitors varied in concentration as appropriate for the particular experiment. Samples were assayed in a 200 μl reaction mixture in a microtitre plate at 30 °C.

Protein concentration was determined by two methods using BSA as standard for each. For routine measurements, the dye-binding method of Sedmak and Grossberg [26] was used. For measurement of the specific activity of pure AHAS, the protein concentration was also determined using a ninhydrin assay of the α-amino content after alkaline hydrolysis of the protein. Nitrogen gas was bubbled through the ninhydrin reagent [75% (v/v) methyl cellosolve, 0.3% hydrindantin, 2% ninhydrin in 1 M sodium acetate pH 5.5] during preparation and just before use. The reagent was stored at 4 °C in the dark and used within 2 weeks. Protein samples were dried down and dissolved in 0.5 ml of 5 M NaOH before hydrolysis of peptide bonds by autoclaving at 121 °C for 20 min. After cooling, 1 ml of 30% acetic acid and 2 ml of ninhydrin reagent were added and mixed. Full colour development was achieved by heating the mixture at 100 °C for 20 min, and, after cooling, the A₅₇₀ of the solution was measured.

Determination of native molecular mass

Native molecular mass of AHAS was determined using a Pharmacia Superose 12 PC column (3.2 mm × 300 mm) coupled to the Pharmacia SMART chromatography system. Thyroglobulin (670 kDa), bovine γ-globulin (158 kDa), chicken ovalbumin (44 kDa), equine myoglobin (17 kDa) and vitamin B₁₂ (1.35 kDa) were used to calibrate the column.

SDS/PAGE

SDS/PAGE was performed using the method of Laemmli [27]. Proteins were separated on a 10% polyacrylamide gel using a Bio-Rad Minigel apparatus and detected by staining with 0.1% Coomassie Blue.

Mass spectrometry

MS analysis of protein was performed using a PE-SCIEX triple quadrupole mass spectrometer equipped with an ion spray atmospheric ionization source. Samples (20 μl) were injected into a Vydac C₁₈ reverse-phase HPLC column (250 mm × 2.1 mm, 5 μm) coupled directly to the ionization source via a fused-silica capillary interface (50 μm internal diameter × 50 cm length). The sample was subjected to an isocratic 0.05% trifluoroacetic acid (TFA) wash for 20 min and subsequently eluted using a stepwise increase from 0.05% TFA to methyl cyanide/0.05% TFA (65:35, v/v). Sample droplets were ionized at a positive potential of 5 kV and entered the analyser through an interface plate and subsequently through an orifice (100–120 mm diameter) at a potential of 80 kV. Full-scan mass spectra were acquired over the mass per charge range of 600–2000 Da with a scan step of 0.1 Da. The spectra were processed with the aid of BioMultiview 1.2 (PE-Sciex).

Sequence determinations

DNA sequencing was performed using the Dye Terminator Cycle Sequencing Ready Reaction Kit (ABI Prism) and DNA Sequencer 373A (Applied Biosystems). For the determination of amino acid sequence, samples were subjected to SDS/PAGE and then blotted on to PVDF membrane. The membrane containing the appropriate protein band was excised and subjected to direct amino acid sequencing by Edman degradation using an automated gas phase sequencer (Applied Biosystems 470A).

Computer programs

Fitting of equations to experimental data was performed using programs based on DNRP53 [28]. The rate equation for the negative co-operative model was derived with the aid of the REFERASS program [29].

RESULTS

Expression and purification

We have tested several constructs to examine the expression of *Arabidopsis* AHAS in *E. coli*. Expression from the initial construct (pTrc99A-AHAS) was demonstrated by its ability to complement growth in minimal medium of the AHAS-deficient *E. coli* strain CU1147. The specific activity of AHAS in the soluble fraction of cell lysate obtained from this and various other constructs is shown in Table 1. We attempted to increase expression levels using various *E. coli* host strains, particularly TOPP[®] cells (from Stratagene) which are claimed to improve expression of eukaryotic proteins. In our hands, there appeared to be no advantage in using these cells (results not shown). We tried adding a C-terminal hexahistidine tag yielding pTrc99A-AHAS(H); this halved the expression level and appeared to offer no benefit in enzyme purification. pND216 is one of a series of heat-inducible

Table 1 Specific activity of *Arabidopsis* AHAS expressed in *E. coli* carrying different AHAS constructs

Cells were grown and induced as described in the Materials and methods section; the soluble fraction of the cell lysate was assayed for protein concentration using the method of Sedmak and Grossberg [26], and AHAS activity was measured using the colorimetric assay.

Construct	Host cell	Specific activity (units/mg of protein)
pTrc99A	CU1147	0.002
pTrc99A-AHAS	CU1147	0.060
pTrc99A-AHAS(H)	CU1147	0.023
pTrc99A-AHAS:I102	CU1147	0.002
pT7-7	BL21(DE3)	0.003
pT7-7-AHAS	BL21(DE3)	0.115
pT7-7-AHAS:T86	BL21(DE3)	0.351
pND216	BL21(DE3)	0.003
pND216-AHAS	BL21(DE3)	0.176

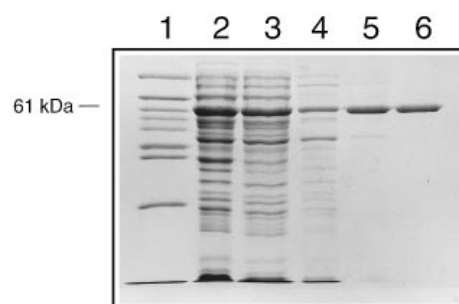
expression vectors [30] with which we have had some success in high-level expression of pyruvate decarboxylase [31]. Putting the coding sequence into this vector tripled the expression.

A doubling of expression was obtained by transferring the coding sequence to the pT7-7 vector and a further tripling resulted from removal of the DNA coding for the first 85 amino acids of the expressed protein. Although the BL21(DE3) host cells used for expression of the pT7-7 vectors is not AHAS-deficient, the level of endogenous enzyme is negligible, accounting for 1–2% of the total activity. Additional removal of N-terminal amino acids beyond Thr-86 up to and including Asp-101 (replaced with the sequence Met-Gly) yields an inactive enzyme as seen with pTrc99A-AHAS:I102. Previously reported values for the specific activity of *Arabidopsis* AHAS (expressed from the intact gene) in the soluble fraction of cell lysate range from 0.037 unit/mg to 0.085 unit/mg [19–21]. Thus our values are comparable with those reported. The level of expression from pT7-7-AHAS:T86 is sufficiently high that purification of the enzyme is achievable from a medium-scale cell culture.

This expressed AHAS has been extensively purified by a procedure involving $(\text{NH}_4)_2\text{SO}_4$ fractionation followed by hydrophobic and anion-exchange chromatography. The purification is summarized in Table 2. The level of AHAS expression seems to improve with the scaling up of the culture, as seen with the higher specific activity in the soluble fraction of cell lysate. The yield of AHAS obtained from this purification procedure was about 22%, with most of the loss occurring in the first anion-exchange chromatography step. The specific activity of the enzyme eventually attained was about 7.8 units/mg, and the final product contains no significant impurities as judged by SDS/PAGE

Table 2 Purification of *Arabidopsis* AHAS expressed from pT7-7-AHAS:T86

Step	Protein (mg)	Activity (units)	Specific activity (units/mg)	Yield (%)
High-speed supernatant	923	886	0.96	100
$(\text{NH}_4)_2\text{SO}_4$ fractionation	740	835	1.13	94
Phenyl-Sepharose	233	791	3.39	89
Macro Prep 50 Q (pH 7.5)	46	299	6.43	33
Macro Prep 50 Q (pH 6.5)	25	197	7.88	22

**Figure 2** SDS/PAGE of *Arabidopsis* AHAS expressed from pT7-7-AHAS:T86 in *E. coli* BL21(DE3) cells

Lane 1, molecular-mass standards; lane 2, soluble fraction of cell lysate; lane 3, after $(\text{NH}_4)_2\text{SO}_4$ precipitation; lane 4, after Phenyl-Sepharose chromatography; lane 5, after Macro-Prep 50 Q (pH 7.5) chromatography; lane 6, after Macro-Prep 50 Q (pH 6.5) chromatography.

(Figure 2). This specific activity was calculated from protein measurements based on a dye-binding assay; this method appears to underestimate the protein concentration by 28% when compared with the ninhydrin assay. Using the latter method, the specific activity is 5.7 units/mg.

The purified enzyme is moderately stable, losing 10% activity after 3 weeks, and 23% after 5 weeks, of storage at 4 °C. At –70 °C, stability is better with losses of 4% (3 weeks, with three freeze–thaw cycles) and 8% (5 weeks, with five freeze–thaw cycles); with no intervening freeze–thaw cycles, only 9–10% activity was lost in 6 months.

We have also purified *Arabidopsis* AHAS expressed from the intact gene in pND216-AHAS, using a similar procedure. In this case, several forms of the enzyme with similar but different molecular masses were observed on SDS/PAGE (results not shown). These different forms co-purified as a single enzyme activity peak in both anion-exchange and gel-filtration chromatography. Attempts to resolve these different forms were not successful.

Physicochemical properties

The apparent molecular mass of AHAS expressed from pT7-7-AHAS:T86 is 61 kDa, which is slightly smaller than the expected size of 63.8 kDa. N-Terminal sequencing yielded the sequence TFISXFAPDQ, indicating that the only processing is removal of the N-terminal methionine. The residue X was tentatively identified as cysteine, although repeated DNA sequencing confirmed the presence of an arginine codon at this particular position. The reason for a cysteine instead of an arginine residue in the N-terminal sequence is not clear. MS gave an absolute mass of 63 864 Da compared with 63 849 Da as calculated from the predicted amino acid sequence, indicating that no major post-translational modification of the protein had occurred. Size-exclusion chromatography of the purified enzyme yielded a single peak corresponding to a molecular mass of 109 kDa which was barely affected (113 kDa) by inclusion of FAD. This size is close to that expected for a dimer.

Kinetic properties

Purified *Arabidopsis* AHAS exhibits maximum activity around neutral pH but the peak is rather broad ranging between pH 6.5 and pH 8.5; a pH of 7.0 was adopted for kinetic studies. Using either the colorimetric or continuous assay methods, there

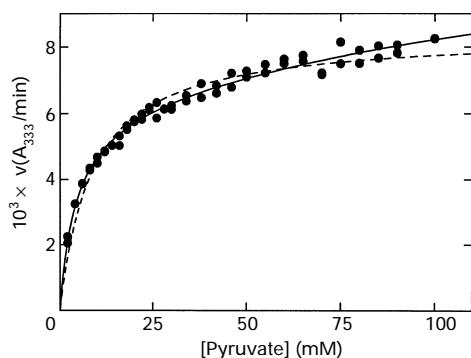
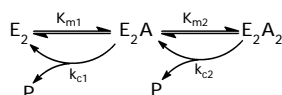


Figure 3 Pyruvate-saturation curve of *Arabidopsis* AHAS

Rates were determined using the continuous assay at the pyruvate concentrations indicated. The solid line shows the best fit of eqn. (1) to the data, which yielded the following values with K_{m2} set at 100 mM: $V_{max} = (13.08 \pm 0.41) \times 10^{-3} A_{333}/\text{min}$, $K_{m1} = 8.01 \pm 0.66$ mM and $R = 0.935 \pm 0.052$. The broken line is the best fit of the Michaelis-Menten equation to the data: $V_{max} = (8.40 \pm 0.10) \times 10^{-3} A_{333}/\text{min}$ and $K_m = 8.48 \pm 0.45$ mM.



Scheme 1 Model for the negatively co-operative substrate kinetics of *Arabidopsis* AHAS

appeared to be a short lag phase of 1–2 min before full activity of the enzyme was attained (results not shown). However, this lag phase could be eliminated by preincubation of the enzyme for several minutes under assay conditions in the absence of substrate.

The effect of pyruvate concentration on the rate of reaction is shown in Figure 3 in which it is seen that the saturation curve does not follow simple Michaelis-Menten kinetics (broken line). Although the departure from a hyperbolic curve is rather subtle and might have been disregarded in a single experiment, it was observed consistently in a large number of experiments. In addition, substrate-saturation curves obtained at different temperatures, pH values and using different buffers yielded curves of a similar shape. This kinetic anomaly is not an artifact arising from possible pH changes from addition of high concentrations of substrate, as the pH of the assay buffer was unaltered by 100 mM pyruvate. Neither does it appear to be due to a non-specific effect of increasing ionic strength, since inclusion of 100 mM NaCl did not affect the activity.

The AHAS reaction requires 2 mol of pyruvate for each mol of acetolactate formed, and this could lead to non-hyperbolic kinetics [12]. However, it would be expected that this would give rise to positive co-operativity, in contrast with the observed data which exhibit negative co-operativity, with a Hill coefficient of 0.603 ± 0.038 . Since AHAS is a dimer, we interpreted these data as arising from interactions between the subunits with substrate binding to the first active site making it harder for binding at the second to occur. This model is depicted in Scheme 1 and includes provision for differences in the catalytic rate constant between the asymmetric (E_2A) and symmetric (E_2A_2) forms. The rate equation for this model is given as eqn. (1), where R is the ratio of catalytic rate constants k_{c1}/k_{c2} .

$$v = V_{max}[A](R K_{m2} + [A]) / (K_{m1} K_{m2} + 2K_{m2}[A] + [A]^2) \quad (1)$$

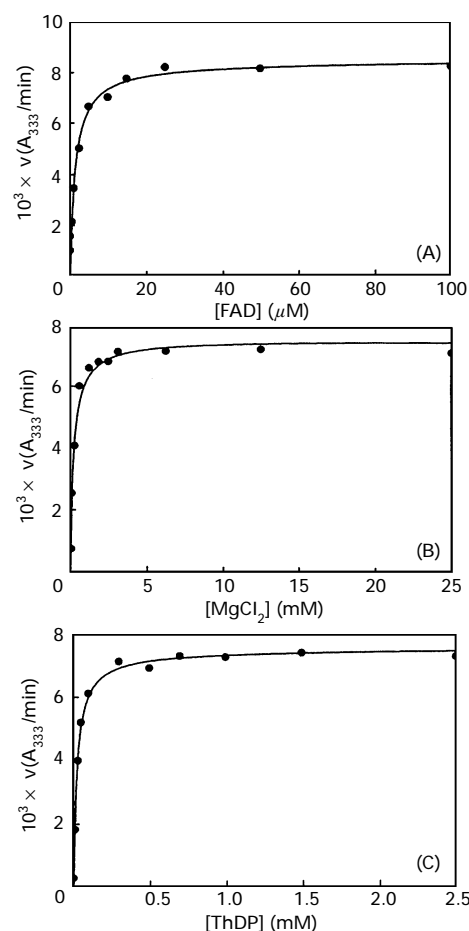


Figure 4 Cofactor-saturation curves of *Arabidopsis* AHAS

Initial rates were measured using the continuous assay with the concentration of one of the cofactors varied as indicated. (A) FAD; (B) Mg^{2+} ; (C) ThDP.

This equation yielded an excellent fit to the data, as shown by the solid line in Figure 3. The K_m for pyruvate at the first active site is 8.01 ± 0.66 mM, but that at the second could not be estimated accurately from the data and was taken to be 100 mM, although other values of the order of 50–200 mM gave similar fits. The estimate of R for these data is 0.935 ± 0.052 , and other data sets usually gave values between 0.65 and 1.15.

Cofactor activation

The effect of each of the cofactors on AHAS was examined. There was little or no observable activity on omission of any one cofactor, and the activation by FAD (Figure 4A), Mg^{2+} (Figure 4B) and ThDP (Figure 4C) followed hyperbolic curves with half-saturating concentrations of 1.46 ± 0.22 , 198 ± 19 and 25.3 ± 1.4 μM respectively.

Inhibition kinetics

The inhibition by each of the three branched-chain amino acids, and a representative of the sulphonylurea and imidazolinone classes of herbicides was assessed. The enzyme was unaffected by valine, leucine or isoleucine at concentrations up to 16 mM (results not shown).

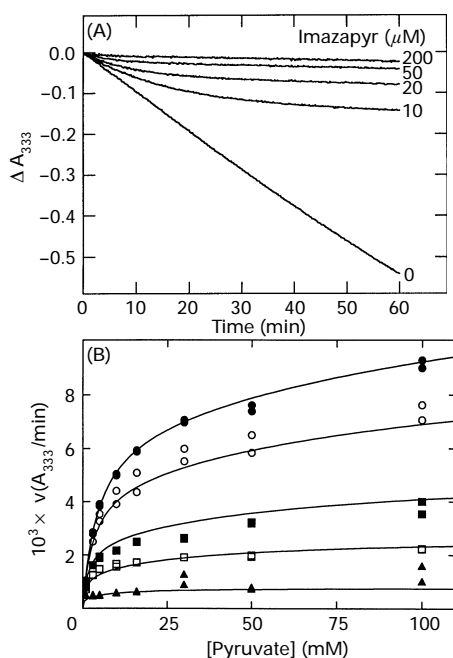


Figure 5 Inhibition of *Arabidopsis* AHAS by imazapyr

(A) Inhibition as a function of time; pyruvate was used at 100 mM, and imazapyr was varied as indicated. (B) Effect of imazapyr on the initial rate. Rates were determined using the continuous assay at the pyruvate concentrations indicated. Imazapyr concentrations used were 0 (●), 5 (○), 20 (■), 50 (□), 100 (not shown) and 200 (▲) μM . The solid lines show the best fit to the data (all five imazapyr concentrations) of the combined eqns. (1) to (4) after eliminating the K_{is1} and K_{is2} terms, with K_{m2} set at 100 mM. This fit yielded the following values: $V_{\max} = (14.71 \pm 0.64) \times 10^{-3} A_{333}/\text{min}$, $K_{m1} = 8.75 \pm 0.89 \text{ mM}$, $R = 1.127 \pm 0.069$ and $K_{ii} = 11.3 \pm 0.5 \mu\text{M}$.

The effect of imazapyr (an imidazolinone) on the activity is illustrated in Figure 5. As shown by the time course of the reaction (Figure 5A), it acts as a slow-binding inhibitor for which the initial relatively weak inhibition becomes progressively stronger during the assay. For example, 50 μM imazapyr gives 54% inhibition initially but this has increased to 95% after 1 h. We have focused our attention on the initial inhibition.

The effect of imazapyr on the initial rate is shown in Figure 5B. The analysis of these data is complex, since the individual pyruvate-saturation curves at each inhibitor concentration do not follow hyperbolic kinetics. To perform this analysis, we used an inhibition model analogous to non-competitive inhibition but based on eqn. (1) rather than an hyperbolic dependence of rate on pyruvate concentration. This model has the form of eqn. (1) but with V_{\max} , K_{m1} and K_{m2} replaced by apparent values defined by eqns. (2) to (4).

$$V_{\max}(\text{app}) = V_{\max}/(1 + [I]/K_{ii}) \quad (2)$$

$$K_{m1}(\text{app}) = K_{m1}(1 + [I]/K_{is1})/(1 + [I]/K_{ii}) \quad (3)$$

$$K_{m2}(\text{app}) = K_{m2}(1 + [I]/K_{is2})/(1 + [I]/K_{ii}) \quad (4)$$

where K_{ii} is an intercept inhibition constant and K_{is1} and K_{is2} are slope inhibition constants. Initial fitting of the data to this model yielded a value of approx. 10 μM for K_{ii} , whereas K_{is1} and K_{is2} were approx. 20-fold higher. This suggests that imazapyr is an uncompetitive inhibitor affecting V_{\max} , K_{m1} and K_{m2} to equal extents. Reanalysis of the data without the slope inhibition constants gave a fit that was not significantly inferior to that for non-competitive inhibition and yielded a value for K_{ii} of $11.3 \pm 0.5 \mu\text{M}$.

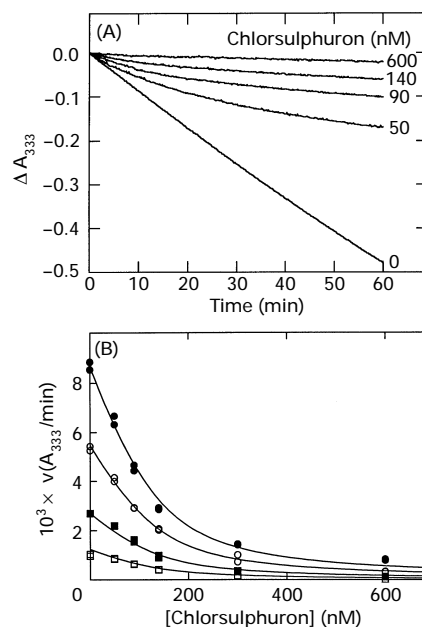


Figure 6 Inhibition of *Arabidopsis* AHAS by chlorsulphuron

(A) Inhibition as a function of time; pyruvate was used at 100 mM, and chlorsulphuron was varied as indicated. (B) Effect of chlorsulphuron on the initial rate. Rates were determined using the continuous assay at the chlorsulphuron concentrations indicated. Pyruvate was used at seven fixed concentrations of 100 (●), 50 (not shown), 30 (not shown), 16 (○), 10 (not shown), 5 (not shown), 3 (■) and 1 (□) mM. The solid lines show the best fit to the data (all seven pyruvate concentrations) of the combined eqns. (1) and (5), with K_{m2} set at 100 mM. This fit yielded the following values: $V_{\max} = (14.49 \pm 0.42) \times 10^{-3} A_{333}/\text{min}$, $K_{m1} = 8.04 \pm 0.51 \text{ mM}$, $R = 0.847 \pm 0.044$ and $K_i(\text{app}) = 32.4 \pm 2.1 \text{ nM}$ and $[E]_0 = 137 \pm 6 \text{ nM}$.

The effect of chlorsulphuron (a sulphonylurea herbicide) is shown in Figure 6; like imazapyr, it is a slow-binding inhibitor. For example 50 nM gives 19% inhibition of the initial rate rising to 86% inhibition after 60 min. This concentration of chlorsulphuron is comparable with the total enzyme concentration ($[E]_0$) used in these assays. Consequently, tight-binding effects must be allowed for, in which combination between chlorsulphuron and the enzyme significantly reduces the free inhibitor concentration. The dependence of rate (v_i) upon total inhibitor concentration ($[I]_0$), adapted from Henderson [32], is given as eqn. (5).

$$v_i^2[E]_0 + v_i v_o ([I]_0 - [E]_0 + K_i(\text{app})) - v_o^2 K_i(\text{app}) = 0 \quad (5)$$

Fitting of eqn. (5) to individual inhibition curves showed that the estimates of both $[E]_0$ and $K_i(\text{app})$ are independent of the pyruvate concentration in the range 1–100 mM, while v_o exhibited the negatively co-operative behaviour described above. The entire data set were then analysed using the combined eqns. (1) and (5); this gave values of V_{\max} , K_{m1} , K_{m2} and R that were similar to those obtained using the data in Figure 3, and the values of $K_i(\text{app})$ and $[E]_0$ obtained from this overall fit were $32.4 \pm 2.1 \text{ nM}$ and $137 \pm 6 \text{ nM}$ respectively.

DISCUSSION

In this report the heterologous expression, purification and characterization of *Arabidopsis* AHAS is described. Purification from a vector expressing the full-length gene gave a mixture of forms of the enzyme that are thought to result from differential cleavage of the AHAS precursor protein by an *E. coli* protease

[20]. This difficulty was solved by expression of the enzyme using a plasmid (Figure 1) from which the chloroplast transit sequence had been removed. Comparison of all the available plant AHAS protein sequences reveals that a high level of sequence homology occurs in the region downstream of the putative transit sequence, and Thr-86 is the first conserved residue. On this basis, residues before Thr-86 were removed from the AHAS gene and a methionine codon was added to provide a start codon for the translation of the AHAS protein. This methionine residue was, however, removed after synthesis of the protein as revealed by N-terminal sequencing. The cleavage site of the plant AHAS transit peptide has not been determined, although speculations of the putative site have been made based on homology (e.g. [33–35]). The cleavage site or sites recognized by the *E. coli* protease may not be identical with that recognized by the plant protease and the presence of more than one cleavage site is also possible, since AHAS purified from wheat leaves exhibits two molecular species of 57 and 58 kDa [18]. Furthermore AHAS from oilseed rape has been shown by immunological detection to contain two types of subunit with molecular masses of 65 and 66 kDa [36]. In contrast, a single polypeptide of approx. 65 kDa was identified in immunoblots of crude extracts from *Arabidopsis* seedlings and in *E. coli* expressing *Arabidopsis* AHAS using antibodies raised against an *Arabidopsis* AHAS fusion protein expressed in *E. coli* [20]. The presence of two subunit sizes of AHAS purified from plants may have resulted from modification of the enzyme during purification. However, these different subunit sizes may also be the result of different cleavage products. Since AHAS is present in very low abundance, it may not be possible to discern small differences of 1–2 kDa when protein from a crude extract is subjected to immunoblot analysis after SDS/PAGE. Even with the bacterial expression system, the level of plant AHAS protein is still very low and is not easily discerned on SDS/PAGE of crude extract. It would be of interest to see whether AHAS purified from *Arabidopsis* seedlings exhibits more than one molecular species on SDS/PAGE. In contrast with plant AHAS, all bacterial forms of the enzyme isolated so far have only a single type of large subunit, as revealed by SDS/PAGE [11,12].

In addition to eliminating the complication of multiple forms of AHAS, removal of the DNA encoding the transit peptide resulted in higher expression levels (Table 1). Similar results have been reported [22] for expression of oilseed rape AHAS in *S. typhimurium* although, in that case, no activity was detected for the full-length sequence. Activity was only detected for two constructs corresponding to deletions that are within a few amino acids of the residue corresponding to *Arabidopsis* Thr-86.

The final specific activity of 7.8 units/mg that we have obtained after purification (Table 2) is the highest that has been reported for any eukaryotic AHAS. Although a somewhat lower value (5.7 units/mg) was obtained when protein was determined using the ninhydrin assay, most of the published specific activities of purified AHAS have been based on dye-binding assays. The only exception is maize AHAS [37] where the protein assay was not stated. With this possible exception, it is with our value of 7.8 units/mg that the published values should be compared. Southan and Copeland [18] obtained the wheat leaf enzyme with a specific activity of only 0.06 unit/mg, maize AHAS was obtained with a specific activity of 0.67 unit/mg [37], while Durner and Böger [17] obtained a preparation of the barley shoot enzyme with a specific activity of 1.6 units/mg and have mentioned preparations with activities as high as 3.1 units/mg [38]. Purification of plant AHAS is hampered by the very low abundance of the enzyme and its instability; the difference in specific activity between the barley and wheat enzyme may be due to loss of activity in the latter.

Purification of eukaryotic AHAS expressed in bacteria has also been difficult because of instability. For example, purified yeast AHAS was reported with an extrapolated specific activity of 5.1 units/mg but, because of instability, the actual specific activity was only 0.17 unit/mg. By protecting the enzyme from light during purification, we have not experienced any such difficulties. The purified enzyme is moderately stable and could be kept at 4 °C for several days with only minor losses (10% in three weeks); for long-term storage, the enzymic activity could be maintained at –70 °C (10% loss in 6 months) provided intervening freeze–thaw cycles were avoided. Recently, Ott et al. [23] described the purification of *Arabidopsis* AHAS, expressed as a GST fusion protein in *E. coli*. Although no mention was made of the stability of their preparation, their final product, after thrombin digestion to excise the GST portion, had a specific activity that is less than one-quarter of that which we have obtained.

In agreement with a previous report [20], *Arabidopsis* AHAS expressed in *E. coli* is insensitive to feedback inhibition by branched-chain amino acids. Possible reasons include the incorrect folding of the enzyme in its native form, incorrect cleavage of the transit peptide and the absence of a small subunit [20]. The requirement of the small subunit for feedback inhibition is feasible, since such a role has been demonstrated for the small subunit of isoenzyme III of *E. coli* AHAS [39]. Evidence for a eukaryotic small subunit is accumulating. Open reading frames for a putative small subunit have been identified in a red alga and in yeast [40], and disruption of this yeast gene affects the sensitivity of yeast AHAS (in crude extracts) to feedback regulation [41]. In addition, expressed sequence tags that may represent portions of AHAS small subunits have been identified recently in rice and *Arabidopsis* (R. G. Duggleby, unpublished work).

A previous study of *Arabidopsis* AHAS in crude extract from seedlings and from *E. coli* expressing the enzyme revealed similar kinetics with respect to pyruvate [20]. The kinetics of the enzyme from both sources were analysed as hyperbolic saturation curves yielding K_m values of 2.3 mM (seedlings) and 2.0 mM (expressed in *E. coli*), although close examination of some of the data reveals deviations from Michaelis–Menten kinetics that are reminiscent of the negative co-operativity that we have observed. In a separate study, Mourad et al. [42] claim to observe strict Michaelis–Menten kinetics of *Arabidopsis* AHAS (from seedlings) with respect to pyruvate, although the data are far from convincing; K_m was estimated to be 6.33 ± 0.17 mM. A K_m for pyruvate as high as 16.8 ± 1.4 mM has been obtained from crude extracts of *E. coli* expressing *Arabidopsis* AHAS [21]; again, small but consistent deviations from a hyperbolic curve are clearly evident in the data. Although the differences in the K_m reported by others could be related to differences in assay conditions, it could also be related to the fact that the substrate-saturation curve is non-hyperbolic. Under these circumstances, the estimated K_m would depend upon the range of substrate concentrations employed for the analysis. Bearing this in mind, the reported K_m values are comparable with our K_{m1} of 8.01 mM: cotton (2.5–6.0 mM [43]), wheat (4 mM [18]), oilseed rape (5 mM [36]), tobacco (6.9–9.6 mM [43]) and *Arabidopsis* (11.2 mM [44]).

Although the non-hyperbolic saturation curve with respect to pyruvate that we have observed (Figure 3) was unexpected, it was observed consistently and we believe that it is real. The deviations from Michaelis–Menten kinetics are quite small and can easily be overlooked, particularly if measurements are restricted to low pyruvate concentrations. As mentioned above, careful examination of published substrate-saturation curves reveals anomalies similar to those that we have seen. We also

band that wheat AHAS has been reported [18] to show a non-hyperbolic pyruvate-saturation curve, although, in this case, the data are described as showing an inflection.

A possible explanation of the negatively co-operative kinetics is that we have a mixture of enzymes with different affinities for the substrate. For example, the data in Figure 3 are consistent with two enzyme forms with approximately equal maximum velocities (4.90×10^{-3} and 5.17×10^{-3} A_{333}/min) but greatly different K_m values (2.87 and 54.1 mM). However, there is no physical evidence to support this suggestion, as we see a single band only on SDS/PAGE, a single peak in gel-filtration chromatography, and a single molecular species by MS. We interpret the negative co-operativity as arising from interactions between the subunits of this dimeric enzyme, whereby substrate binding at one active site reduces the affinity for binding at the second (Scheme 1). The crystal structures of four ThDP-dependent enzymes have been determined, and in all cases the active site lies at the dimer interface and the same is likely to be true for AHAS. This fact provides a possible mechanism for the negative co-operativity; substrate binding at one active site could perturb the dimer interface and thereby transmit a structural change to the second active site making binding of the substrate more difficult. Alternatively, Nikkola et al. [45] have suggested that a proton channel exists between the two active sites of transketolase and, if present in AHAS, could provide a molecular mechanism for the negative co-operativity.

None of the cofactors is tightly bound, judging from the observation that little or no activity was seen upon omission of each of the cofactors from the assay (Figure 4). Even FAD, which was included in all the buffers used in purification, appears to be lost easily despite its high affinity ($K_m = 1.46 \mu\text{M}$). Unlike the barley enzyme, which aggregates in the presence of FAD [46], *Arabidopsis* AHAS remains dimeric in the presence of this cofactor. It is usual to add FAD to the assay, suggesting that, as we observe, this cofactor is required. Singh et al. [3] reported substantial activity without added FAD in crude extracts from maize cell culture but, as the authors acknowledge, these extracts contained $100 \mu\text{M}$, so carry-over into the assay cannot be excluded. The affinity of *Arabidopsis* AHAS for ThDP ($25.3 \mu\text{M}$) is similar to that reported for the maize ($12.4 \mu\text{M}$ [47]), tobacco ($20\text{--}42 \mu\text{M}$ [44]) and cotton ($32\text{--}49 \mu\text{M}$ [44]) enzymes but otherwise there are few data in the literature on cofactor activation of plant AHAS. Singh et al. [3] report little activity without added ThDP or Mg^{2+} , and 'saturation' by 0.5 and 1 mM concentrations of these cofactors respectively.

It has been reported previously that the sulphonylurea herbicides are slow- and tight-binding inhibitors of AHAS (e.g. [48]). Inhibition of *Arabidopsis* AHAS by chlorsulphuron also exhibited slow- and tight-binding kinetics (Figure 6). The inhibition constant for chlorsulphuron was obtained only for the initial phase of the inhibition. The $K_i(\text{app})$ of 32.4 nM is similar in magnitude to the value of 68 nM obtained for the barley enzyme [49]. Inhibition of the barley enzyme by chlorsulphuron was shown to be non-competitive, with the slope and intercept of a double-reciprocal plot almost equally affected by the inhibitor. This implies that the $K_i(\text{app})$ would be unaffected by the substrate concentration [50], which is what we have found for *Arabidopsis* AHAS. We suggest that the inhibition that we observe is non-competitive, although the complexity of the data, with tight-binding inhibition superimposed on non-hyperbolic substrate kinetics, makes interpretation difficult. These complexities limit the usefulness of comparisons with published data, particularly when the literature values (usually reported as an IC_{50}) do not clearly distinguish between effects on initial rates and rates obtained as an average from a prolonged incubation with

inhibitor. Nevertheless, there is broad agreement that the sulphonylureas inhibit in the nanomolar concentration range: barley (chlorsulphuron 33–34 nM [49]), *Arabidopsis* (chlorsulphuron 2–2.1 nM [20], metsulphuron methyl 80 nM [21]), wheat (chlorsulphuron 600 nM, metsulphuron methyl 300 nM [18]) and several plant species (chlorsulphuron 11–32 nM, metsulphuron methyl 9–46 nM [51]).

Analysis of the data in Figure 6(B) gave an active-site concentration of 137 nM, and this raises a curious point in relation to Figure 6(A), from which it is seen that 50 nM chlorsulphuron gives 86% inhibition after 60 min. If each molecule of chlorsulphuron completely inhibited one active site, then it would be expected to give 36% inhibition at most. Even if each molecule of chlorsulphuron completely inhibited both active sites in the dimer, the inhibition should not exceed 73%. There have been reports [52] that treatment of whole plants with these herbicides results in an irreversible loss of extractable AHAS activity, although the amount of AHAS protein (detected immunologically) is unchanged [53]. In contrast, inhibitor binding *in vitro* appears to be reversible [37]. This apparent conflict was investigated by Durner et al. [49], who showed that the irreversible inactivation occurs under turnover conditions (as would occur *in vivo* and in the experiment illustrated in Figure 6A), and that release of bound herbicide is not accompanied by a corresponding increase in AHAS activity. Thus it appears that herbicides could bind to the enzyme, promote inactivation, then be released and available to cause inactivation of further enzyme molecules. The data in Figure 6 provide some support for this proposal, although more direct experiments would be needed to provide convincing evidence.

With imazapyr, the inhibition kinetics were somewhat less complex (Figure 5) in that tight-binding is not a factor. The inhibitor appeared to affect V_{max} and the two K_m values to equal extents; for an enzyme exhibiting Michaelis–Menten kinetics, this would result in a change in the $1/v$ intercept only of a double-reciprocal plot (uncompetitive inhibition). Apparent K_i values (or IC_{50} values) for imidazolinone herbicides have been reported for AHAS from various plants. In most cases these were determined at a fixed pyruvate concentration in an assay that would not permit true initial rates to be determined. Consequently, these values are not strictly comparable with the K_i of $11.3 \mu\text{M}$ that we have measured. Nevertheless, they are all of a similar magnitude: maize (imazapyr 5.0–12.3 μM [54]; imazaquin 12 μM [49]), wheat (imazaquin 2.5 μM , imazethapyr 5 μM , imazaquin 10 μM [18]), barley (imazaquin 3.8–6 μM [49]) and *Arabidopsis* (imazethapyr, 2 μM [20]). Some workers have recognized that the inhibition is time-dependent and have attempted to determine an initial K_i . This parameter should be more similar to what we have measured, and the reported values for maize (imazapyr, 15 μM [37]) and barley (imazaquin 10 μM [49]) agree well. In this latter case, the kinetics of inhibition have been determined and are reported to be uncompetitive [49] as we observe. However, the K_i value of 10 μM (imazaquin) cannot be compared directly with our value (11.3 μM imazapyr) because of the difference in herbicide.

In conclusion, we have obtained good expression of *Arabidopsis* AHAS in *E. coli* by cloning the gene into pT7-7 after removing the DNA that encodes the chloroplast transit sequence. The enzyme has been purified to a specific activity of 7.8 units/mg, the highest value yet reported for any eukaryotic AHAS. Activity is absolutely dependent on the three cofactors FAD, ThDP and Mg^{2+} . The substrate-saturation curve displays negatively co-operative kinetics, which we believe results from interactions between the subunits of this dimeric enzyme. AHAS is not inhibited by the branched-chain amino acids but shows

time-dependent inhibition by herbicides. We have examined the effect of these herbicides on initial rates; it is uncompetitively inhibited by imazapyr ($K_i = 11 \mu\text{M}$) and non-competitively by chlorsulphuron ($K_i = 32 \text{nM}$).

REFERENCES

- 1 Umbarger, H. E. (1975) in *Synthesis of Amino Acids and Proteins* (Arbstein, H. R. V., ed.), pp. 1–56. MTP International Review of Science, Butterworths, London
- 2 Davies, M. E. (1963) *Plant Physiol.* **39**, 53–59
- 3 Singh, B. K., Stidham, M. A. and Shaner, D. L. (1988) *Anal. Biochem.* **171**, 173–179
- 4 Muller, Y. A., Lindqvist, Y., Furey, W., Schulz, G. E., Jordan, F. and Schneider, G. (1993) *Structure* **1**, 95–103
- 5 Chaleff, R. S. and Mauvais, C. J. (1984) *Science* **224**, 1443–1445
- 6 Schloss, J. V., Ciskanik, L. M. and Van Dyk, D. E. (1988) *Nature (London)* **331**, 360–362
- 7 Subramanian, M. V., Loney-Gallant, V., Dias, J. M. and Mireles, M. C. (1991) *Plant Physiol.* **96**, 310–313
- 8 Mourad, G. and King, J. (1992) *Planta* **188**, 491–497
- 9 Schloss, J. V. and Van Dyk, D. E. (1988) *Methods Enzymol.* **166**, 445–454
- 10 Grimminger, H. and Umbarger, H. E. (1979) *J. Bacteriol.* **137**, 846–853
- 11 Eoyang, L. and Silverman, P. M. (1984) *J. Bacteriol.* **157**, 184–189
- 12 Schloss, J. V., Van Dyk, D. E., Vasta, J. F. and Kutny, R. M. (1985) *Biochemistry* **24**, 4952–4959
- 13 Barak, Z., Calvo, J. M. and Schloss, J. V. (1988) *Methods Enzymol.* **166**, 455–458
- 14 Ryan, E. D. and Kohlhaw, G. B. (1974) *J. Bacteriol.* **120**, 631–637
- 15 Poulsen, C. and Stougaard, P. (1989) *Eur. J. Biochem.* **185**, 433–439
- 16 Falco, C., Dumas, K. S. and Livak, K. J. (1985) *Nucleic Acids Res.* **13**, 4011–4027
- 17 Durner, J. and Böger, P. (1988) *Z. Naturforsch.* **43c**, 850–856
- 18 Southan, M. D. and Copeland, L. (1996) *Physiol. Plant.* **98**, 824–832
- 19 Smith, J. K., Schloss, J. V. and Mazur, B. J. (1989) *Proc. Natl. Acad. Sci. U.S.A.* **86**, 4179–4183
- 20 Singh, B., Szamosi, I., Hand, J. M. and Misra, R. (1992) *Plant Physiol.* **99**, 812–816
- 21 Kim, H.-J. and Chang, S.-I. (1995) *J. Biochem. Mol. Biol.* **28**, 265–270
- 22 Wiersma, P. A., Hachey, J. E., Crosby, W. L. and Moloney, M. M. (1990) *Mol. Gen. Genet.* **224**, 155–159
- 23 Ott, K.-H., Kwagh, J.-G., Stockton, G. W., Sidorov, V. and Kekefuda, G. (1996) *J. Mol. Biol.* **263**, 359–368
- 24 Hattori, J., Rutledge, R., Labbé, H., Brown, D., Sunohara, G. and Miki, B. (1992) *Mol. Gen. Genet.* **232**, 167–173
- 25 Sambrook, J., Fritsch, E. F. and Maniatis, T. (1989) *Molecular Cloning: A Laboratory Manual*, (2nd edn.), Cold Spring Harbor Laboratory Press, Cold Spring Harbor, NY
- 26 Sedmak, J. J. and Grossberg, S. E. (1977) *Anal. Biochem.* **79**, 544–552
- 27 Laemmli, U. K. (1970) *Nature (London)* **227**, 680–685
- 28 Duggleby, R. G. (1984) *Comput. Biol. Med.* **14**, 447–455
- 29 Varon, R., Garcia-Sevilla, F., Garcia-Moreno, M., Garcia-Canovas, F., Peyro, R. and Duggleby, R. G. (1997) *Comput. Appl. Biosci.* **13**, 159–167
- 30 Elvin, C. M., Thompson, P. R., Argall, M. E., Hendry, P., Stamford, N. P., Lilley, P. E. and Dixon, N. E. (1990) *Gene* **87**, 123–126
- 31 Candy, J. M., Koga, J., Nixon, P. F. and Duggleby, R. G. (1996) *Biochem. J.* **315**, 745–751
- 32 Henderson, P. J. F. (1973) *Biochem. J.* **127**, 321–333
- 33 Mazur, B. J., Chui, C.-F. and Smith, J. K. (1987) *Plant Physiol.* **85**, 1110–1117
- 34 Rutledge, R. G., Ouellet, T., Hattori, J. and Miki, B. L. (1991) *Mol. Gen. Genet.* **229**, 31–40
- 35 Grula, J. W., Hudspeth, R. L., Hobbs, S. L. and Anderson, D. M. (1995) *Plant. Mol. Biol.* **28**, 837–846
- 36 Bekkaoui, F., Schorr, P. and Crosby, W. L. (1993) *Physiol. Plant.* **88**, 475–484
- 37 Muhitch, M. J., Shaner, D. L. and Stidham, M. A. (1987) *Plant Physiol.* **83**, 451–456
- 38 Durner, J., Gailus, V. and Böger, P. (1994) *FEBS Lett.* **354**, 71–73
- 39 Vyzamensky, M., Sella, C., Barak, Z. and Chipman, D. E. (1996) *Biochemistry* **35**, 10339–10346
- 40 Duggleby, R. G. (1997) *Gene* **190**, 245–249
- 41 Cullin, C., Baudinbaillieu, A., Guillemet, E. and Ozierkalogeropoulos, O. (1996) *Yeast* **12**, 1511–1518
- 42 Mourad, G., Williams, D. and King, J. (1995) *Planta* **196**, 64–68
- 43 Subramanian, M. V., Hung, H.-Y., Dias, J. M., Miner, V. W., Butler, J. H. and Jachetta, J. J. (1990) *Plant Physiol.* **94**, 239–244
- 44 Wu, K., Mourad, G. and King, J. (1994) *Planta* **192**, 249–255
- 45 Nikkola, M., Lindqvist, Y. and Schneider, G. (1994) *J. Mol. Biol.* **238**, 387–404
- 46 Durner, J. and Böger, P. (1990) *Plant Physiol.* **93**, 1027–1031
- 47 Roux, C., Delfourne, E. and Bastide, J. (1996) *Plant Physiol. Biochem.* **34**, 293–299
- 48 LaRossa, R. A. and Schloss, J. V. (1984) *J. Biol. Chem.* **259**, 8753–8757
- 49 Durner, J., Gailus, V. and Böger, P. (1991) *Plant Physiol.* **95**, 1144–1149
- 50 Duggleby, R. G. (1988) *Biochem. Med. Metab. Biol.* **40**, 204–212
- 51 Ray, T. B. (1986) *Trends Biochem. Sci.* **11**, 180–183
- 52 Shaner, D. L., Singh, B. K. and Stidham, M. A. (1990) *J. Agric. Food Chem.* **38**, 1279–1282
- 53 Shaner, D. L. and Singh, B. K. (1991) *Plant Physiol.* **97**, 1339–1341
- 54 Singh, B. K. and Schmitt, G. K. (1989) *FEBS Lett.* **258**, 113–115